

TOTAL CROSS SECTIONS OF  $\pi^+$ ,  $K^+$  AND  $p$  ON PROTONS AND DEUTERONS  
IN THE MOMENTUM RANGE 15-60 GeV/c

S. P. DENISOV, S. V. DONSKOV, Yu. P. GORIN, A. I. PETRUKHIN, Yu. D. PROKOSHKIN  
D. A. STOYANOVA, J. V. ALLABY\* and G. GIACOMELLI\*\*  
*Institute of High Energy Physics, Serpukhov, U.S.S.R.*

Received 30 July 1971

Total cross-section data are presented for protons, positive pions and positive kaons on protons and deuterons in the momentum range 15 GeV/c to 60 GeV/c in 5 GeV/c steps.

This letter gives the first results of total cross-sections for positive particles measured at the 70 GeV proton synchrotron of the Institute for High Energy Physics. The data presented are for  $p$ ,  $\pi^+$  and  $K^+$  in the momentum range 15 GeV/c to 60 GeV/c on hydrogen and deuterium. The standard transmission technique was employed, and the experiment utilized essentially the same detection equipment as used in the earlier measurements of cross-sections for negative particles [1,2].

Positive particles produced in an internal target of the synchrotron were extracted using a magnetic shielding at angles ranging from 10-50 mrad depending on momentum [3,4]. For secondary momenta between 25 and 60 GeV/c the target was operated on the full energy flattop of the accelerator, i.e. using incident protons of 70 GeV. For the measurements at 15 and 20 GeV/c the target was operated on a "front porch" at 35 GeV. The beam transport system, apart from a realignment of the first four quadrupoles, was identical with that used for the earlier measurements with negative particles [1,2].

For the measurements on protons and kaons, the monitor consisted of signals from scintillation counters defining the beam, the differential counter [5] tuned to the desired particles, and the threshold counter [6] which detected all lighter particles and was used in anticoincidence. Contamination of unwanted particles was always smaller than 0.1%. For the measurements on pions, the threshold counter was in coincidence. The total flux in the beam was kept always

smaller than  $10^5$  per burst with a spill time of  $\sim 1$  sec.

The transmission counters were the same as used in the previous measurements and were moved along the beam line, downstream of the targets, such that at each momentum, the solid angle subtended by the transmission counters accepted the same range of four-momentum transfer squared. This procedure, which was done to avoid energy-dependent systematic errors in the extrapolation of partial cross-sections to  $t = 0$ , was identical to that carried out in the earlier experiments with negative particles [1,2].

The new element in this experiment, in comparison with previous measurements [2], was the target system. The target cells used were cylinders, 1.5 m long and 12 cm diameter, one containing liquid hydrogen and the other liquid deuterium. This provided  $10.9 \text{ g/cm}^2$  hydrogen and  $26.3 \text{ g/cm}^2$  of deuterium in the path of the beam. The liquid hydrogen was essentially pure para-hydrogen (less than 5% ortho); the liquid deuterium was in the n-state. The total thickness of the mylar end windows of the target cells and vacuum vessel was 1.2 mm. An identical evacuated dummy target was used for the empty target measurements. The target lengths were measured under the experimental conditions (i.e. full of liquid  $H_2$  and  $D_2$ ) by an optical technique which also measured the profile of the windows of the target. A small correction ( $\sim 0.1\%$ ) was applied for the curvature of the ends of the targets. The target lengths were known with an accuracy of 0.6 mm, i.e. 0.04%.

Throughout the experiment, the vapour pressures of the hydrogen and deuterium cells were monitored by precision manometers to an accu-

\* Visitor from CERN, Geneva, Switzerland.

\*\* Visitor from University of Bologna and INFN, Bologna, Italy.

Table 1.

Estimated values of  $\rho$ , the ratio of the real to imaginary parts of the forward scattering amplitude, used in the computation of the Coulomb-nuclear interference correction  $\delta_{CN}$ , and the effect of the combined correction  $(\delta_C + \delta_{CN})$  on the total cross-sections.

Momentum GeV/c	$-\rho$			$-(\delta_C + \delta_{CN})$ mb					
	pp	$\pi^+p$	$K^+p$	pp	$\pi^+p$	$K^+p$	pd	$\pi^+d$	$K^+d$
15	0.24	0.18	0.22	0.20	0.08	0.08	0.35	0.14	0.16
20	0.21	0.15	0.18	0.18	0.07	0.06	0.32	0.13	0.13
25	0.18	0.14	0.16	0.16	0.07	0.06	0.28	0.12	0.12
30	0.16	0.12	0.14	0.14	0.07	0.05	0.24	0.10	0.11
35	0.15	0.11	0.12	0.13	0.06	0.05	0.23	0.09	0.10
40	0.14	0.10	0.11	0.12	0.06	0.05	0.21	0.08	0.09
45	0.13	0.09	0.10	0.11	0.05	0.04	0.19	0.08	0.09
50	0.12	0.08	0.09	0.11	0.05	0.04	0.18	0.07	0.08
55	0.11	0.07	0.09	0.10	0.05	0.03	0.17	0.07	0.07
60	0.10	0.06	-	0.10	0.04	-	0.16	0.07	-

Table 2.

Results of the total cross-section measurements. The statistical error is given for each point. The systematic scale errors are indicated at the foot of the table.

Momentum GeV/c	$\sigma_{tot}$			$\sigma_{tot}$			$\sigma_{tot}$		
	pp	$\pi^+p$	$K^+p$	pd	$\pi^+d$	$K^+d$	pn	$\pi^+n$	$K^+n$
15	39.29±0.12	24.08±0.12	17.31±0.13	75.25±0.22	48.21±0.22	34.44±0.20	39.68±0.17	25.60±0.20	17.87±0.23
20	39.06±0.12	23.52±0.11	17.42±0.16	74.48±0.22	47.15±0.22	34.61±0.23	39.06±0.17	25.03±0.20	17.94±0.28
25	38.80±0.12	23.43±0.11	17.68±0.10	74.00±0.22	46.85±0.22	34.71±0.20	38.79±0.20	24.85±0.23	17.78±0.18
30	38.59±0.12	23.32±0.11	17.72±0.10	73.85±0.22	46.41±0.22	34.66±0.20	38.84±0.15	24.45±0.20	17.69±0.18
35	38.49±0.12	23.06±0.11	17.80±0.10	73.53±0.22	45.91±0.22	35.15±0.20	38.58±0.24	24.18±0.22	18.12±0.18
40	38.50±0.12	23.08±0.11	18.05±0.13	73.60±0.22	45.21±0.30	35.42±0.20	38.65±0.15	23.42±0.30	18.15±0.22
45	38.45±0.12	23.14±0.12	17.88±0.12	73.22±0.22	45.88±0.22	35.40±0.20	38.28±0.15	24.07±0.23	18.30±0.24
50	38.46±0.12	23.11±0.12	18.37±0.11	73.43±0.22	45.51±0.22	35.60±0.20	38.50±0.23	23.71±0.25	18.02±0.20
55	38.43±0.12	23.14±0.12	18.17±0.14	73.26±0.22	45.65±0.22	35.80±0.20	38.35±0.22	23.83±0.22	18.43±0.24
60	38.44±0.12	23.33±0.20	-	73.42±0.22	45.58±0.40	-	38.51±0.19	23.56±0.40	-
Systematic scale error	±0.4%	±0.5%	±0.4%	±0.5%	±0.6%	±0.5%	±1.8%	±1.4%	±1.3%

racy of 1 mm Hg. The value of the temperature of the hydrogen cell was evaluated from the absolute vapour pressure using the tables of Tapper [7]. The temperature of the deuterium cell was assumed to be equal to the temperature of the hydrogen cell. The average value of the temperature throughout the experiment was 20.28°K and the variations from this value were normally less than 0.05°K with a maximum variation of 0.1°K observed for a short period when the atmospheric pressure was abnormally low. Thus for all the data, the density was constant to within less than ±0.1%. From the values of the temperature the molar volume of both hydrogen and deuterium was calculated, using the tables of Tapper [7]. The deuterium density was corrected for (1.8±0.6)% hydrogen contamination,

mainly in the form of HD molecules, determined by a mass spectrometer technique and by a precise measurement of the gas density. Both methods gave the same results within errors.

The final value of the target thickness in gm cm<sup>-2</sup> was estimated to have a point to point error of much less than 0.1%. The systematic scale errors arising from the uncertainty in the tables [7], the error in temperature determination, the uncertainty in the target length and the error in the estimate of contaminations have been estimated to be 0.1% for hydrogen and 0.3% for deuterium.

The data were taken in a single period of accelerator operation lasting three weeks. Periodically, proton cross-sections at 30 GeV/c were remeasured as a check on reproducibility which

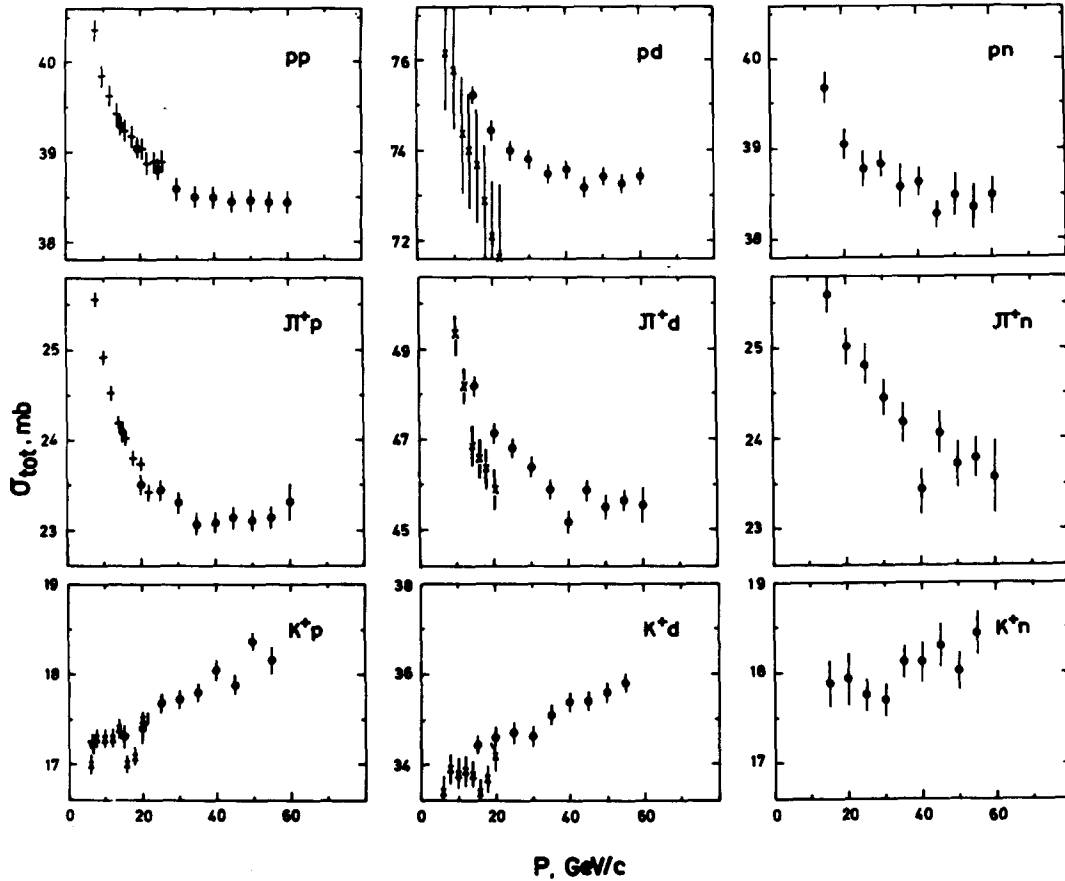


Fig. 1. Results of the total cross-section measurements for positive particles. The new data [ $\diamond$ ] are compared with the lower energy data of Foley et al. [13] [ $+$ ], Galbraith et al. [14] [ $\times$ ], and Beupre et al. [15] [ $\nabla$ ]. The errors shown are statistical only.

was better than 0.1%. At each momentum a standard procedure for setting the beam elements and tuning the Cerenkov counters was followed. Cross-section measurements consisted of a series of runs where the particles transmitted through the target and detected by each transmission counter were recorded for a fixed number of monitor counts [1,2]. The series of runs was a cyclic permutation of measurements with hydrogen, deuterium, and dummy targets. At the end of each run, the data were transferred onto punched cards for off-line analysis, which was carried out on a BESM-6 computer. Data were scrutinized to check that channel efficiencies were good ( $\geq 99.8\%$ ).

The delayed coincidences of the transmission counters were continuously recorded and were used to measure the variations in instantaneous beam rate. The dependence of the measured cross-

sections on beam rates was studied and the effect was found to be correlated with the delayed coincidence rate. Under standard conditions in the 25 to 60 GeV/c momentum region, the value of the delayed coincidences was  $\sim 0.5\%$ , which corresponded to a correction of 0.15% to the cross-sections. At 15 and 20 GeV/c secondary momentum, the delayed coincidences were much larger because of the R.F. structure contained in the beam, and in the largest counters reached values of 2-5%. This corresponded to a correction which was a maximum of 1% at 20 GeV/c.

The extrapolation to zero solid angle was carried out using the relation

$$\sigma(t_i) = \sigma_{\text{tot}} \exp(at_i + bt_i^2) \quad (1)$$

where  $\sigma(t_i)$  is the partial cross-section measured by the  $i$ th channel accepting a maximum four-momentum squared  $t_i$ , and  $\sigma_{\text{tot}}$  is the de-

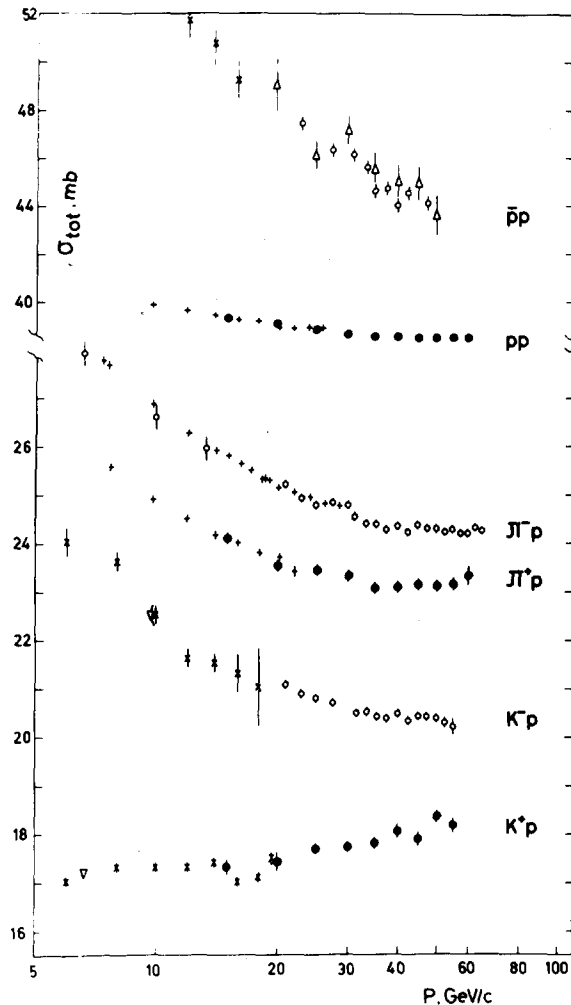


Fig. 2. Comparison of total cross-sections for  $K^{\pm}p$ ,  $\pi^{\pm}p$ ,  $pp$  and  $\bar{p}p$  reactions. The data are from this experiment [ $\diamond$ ]; Allaby et al. [1] [ $\diamond$ ]; Denisov et al. [2] [ $\diamond$ ]; Foley et al. [13] [ $+$ ]; Galbraith et al. [14] [ $\times$ ]; and Beupre et al. [15] [ $\diamond$ ]. The errors shown are statistical only.

sired total cross-section [1]. This form gave statistically acceptable fits to the data in the  $t$ -range used, which was  $0.014 < |t_i| < 0.065$   $(\text{GeV}/c)^2$ . The first two transmission counters ( $|t_i| < 0.01$   $(\text{GeV}/c)^2$ ) were usually ignored because of Coulomb scattering effects. The extrapolation  $t$ -range was varied by adding and subtracting one counter at the beginning and end of the range in order to check the stability of the extrapolated cross-section.

The values of the parameter  $a$  in eq. (1) were found to be constant or smoothly varying over the

momentum range studied. For the deuterium data with all particles, the parameter  $b$  was normally positive and reasonably well determined although for  $K^+d$  the difference from zero was not very significant. For the hydrogen data,  $b$  was definitely positive and fairly well determined for protons. For  $\pi^+p$  the value of  $b$  was normally positive but not very significantly different from zero. For  $K^+p$ ,  $b$  was found to be varying in sign and always statistically consistent with zero.

Extrapolations were also made without the quadratic term in eq. (1), i.e. with  $b=0$ . As might be expected the difference between the value obtained by the quadratic fit and the linear fit reflected the effect of the quadratic term through the magnitude of the  $b$  coefficient. Thus for the data on the proton-proton cross-sections, the quadratic exponential fit gave a resultant cross-section about 0.5% higher than the linear fit, whereas for  $\pi^+$  on hydrogen the difference was small and changed sign at some momenta. The data for  $K^+$  on hydrogen gave differences usually smaller than the statistical errors and with no definite sign.

Hence in the final values quoted, the quadratic exponential fit has been adopted for all the data with the exception of  $K^+$  on hydrogen where the linear exponential fit was used. However, in a few cases the quadratic fit for  $\pi^+p$  or  $K^+d$  resulted in a negative coefficient  $b$ . In these cases a fit was made using a positive value of  $b$ , obtained by interpolation from neighbouring momenta.

The pion cross-sections were corrected for muon contamination in the beam. The contamination was measured directly at 20 and 30  $\text{GeV}/c$  by utilizing the high resolution threshold Cerenkov counter and the coincidence signal  $S_6S_7$  from the two counters behind the steel at the end of the beam [1,2]. The small correction arising from pion decay between the threshold counter and the center of the target was computed and added to the measured contamination to yield the total  $\mu^+$  contamination.

Another measurement of the  $\mu^+$  contamination was obtained by measuring the cross-section with the counters  $S_6S_7$  in coincidence with the transmission counters, but not in the monitor [2]. This has the effect of artificially increasing the fraction of  $\mu^+$  in the beam at the target, since the beam can be considered as composed of only those  $\pi^+$  which decay after the target and produce a muon which can be detected in  $S_6S_7$ . The decay probability was about 1%, independent of momentum, so these measurements yielded a cross-section lower than the real  $\pi^+$  cross-section, by

an amount corresponding to a  $\mu^+$  contamination 100 times greater than in the  $\pi^+$  cross-section measurements. Hence even with a rather crude measurement of this type, it was possible to find the muon contamination with a good accuracy.

Measurements of the muon correction by the last method were made at all momenta. At 20 and 30 GeV/c, these values agreed with the direct measurement made with the threshold Cerenkov counter. The muon contamination varied from 2.5% at 15 GeV/c to 1.0% at 60 GeV/c. The systematic error assigned to this correction was 0.3%, with a point to point error of 0.1%.

The effect of material in the beam path was investigated by measuring the total cross-section with additional material placed at different points along the beam. A correction of  $(0.2 \pm 0.1)\%$  was applied to all the total cross-sections to allow for the residual matter in the beam (scintillators, windows, air, etc.).

The final data were corrected for the combined effect of Coulomb scattering and Coulomb-nuclear interference neglecting the effects of spin. In order to evaluate the latter, the value of the ratio of the real to imaginary part of the scattering amplitude  $\rho$  is needed. For pp scattering this has been measured [8,9], but for  $\pi^+$ p and  $K^+$ p it was estimated, using a Regge model [10]. An error was assigned to these values of  $\rho$  of 0.05. This corresponds to an error in the total cross-section of less than 0.1%.

For the total cross-sections on deuterium the Coulomb correction  $\delta_C$  and the Coulomb-nuclear interference correction  $\delta_{CN}$  can be estimated using a formula which considers elastic scattering and deuteron break-up [9]. However because of the largely unknown forward real parts for scattering on neutrons,  $\delta_{CN}$  is poorly determined. It was finally assumed to be equal to 1.5 times the hydrogen correction for  $\pi^+$ d and two times the hydrogen correction for pd and  $K^+$ d.

The corrections  $\delta_C$  and  $\delta_{CN}$  were evaluated as a function of the accepted  $t$ -range of each transmission counter. Then the corrections were added and applied to each partial cross-section,  $\sigma(t_i)$ , before the final extrapolation. Table 1 shows the effect of the combined corrections on the total cross-sections as well as the estimated values of  $\rho$  used in the computation. Beam size effects, investigated by means of a Monte-Carlo calculation, were found to yield effects smaller than 0.1% and so were negligible.

From the total cross-sections on deuterium and hydrogen the total cross-sections on neutrons have been derived, using the Glauber for-

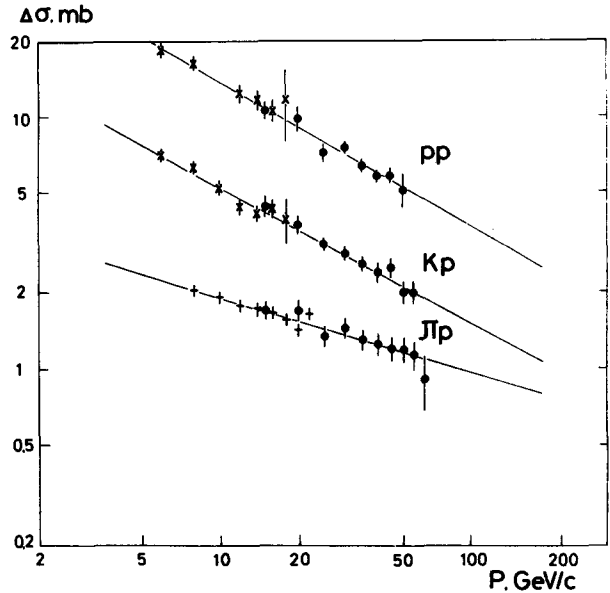


Fig. 3. Values of the total cross section differences,  $\Delta\sigma = \sigma^- - \sigma^+$ , for  $K^+p$ ,  $\pi^+p$ , and  $p^+p$  reactions. The three straight lines are least-squares fits to the data of the form  $\Delta\sigma = Ap^{-n}$  where  $p$  is the incident momentum in GeV/c. The best-fit values of  $A$  and  $n$  are given in table 3.

mula [11] to take into account the shadow effect, neglecting the Fermi motion

$$\sigma_n = \sigma_d - \sigma_p + \delta \tag{2}$$

where the shadow terms  $\delta$  is given by

$$\delta = \frac{\langle r^{-2} \rangle}{4\pi} \sigma_p \sigma_n \tag{3}$$

The real parts of the forward scattering amplitude have been neglected in eq. (3) since they are estimated to be small.  $\langle r^{-2} \rangle$  is the mean inverse square separation between the proton and the neutron in the deuteron. In the present work a value  $0.030 \text{ mb}^{-1}$  has been used and an error of  $\pm 0.005 \text{ mb}^{-1}$  has been assigned to it, just as was done with the equivalent data for negative particles [1]. In other words  $\langle r^{-2} \rangle$  was assumed to be independent of the incident momentum. However, several authors [12] have suggested that  $\langle r^{-2} \rangle$  might depend on the momentum.

The results for the cross-sections obtained in this experiment are shown in table 2, where the first column gives the total cross-sections on hydrogen, the second column the cross-sections on deuterium, and the final column shows the cross-sections on neutrons derived using the

Table 3.

Values of the parameters of the least-squares fit of the form  $\Delta\sigma = A p^{-n}$  to the cross-section differences shown in fig. 3.

	$p^+p$	$K^+p$	$\pi^+p$
$A(\text{mb})$	$56.8 \pm 5.3$	$19.2 \pm 1.3$	$3.88 \pm 0.35$
$n$	$0.61 \pm 0.03$	$0.56 \pm 0.02$	$0.31 \pm 0.04$

Glauber formula (2). The systematic scale error shown at the foot of table 2 comprises the uncertainties in the target thicknesses, the error assigned to the extrapolation procedure, the uncertainty of the corrections for material in the beam and rate dependent effects, and the overall uncertainty of the muon correction applied to the  $\pi^+$  cross-sections. The systematic error for the neutron cross-sections also includes the error in the Glauber correction.

The new results are compared with existing data [13-15] in fig. 1. In the regions of overlap with data at lower momenta, the new results give satisfactory agreement. (Systematic scale errors are not shown in fig. 1).

In the higher momentum region the most interesting and unique feature is the increase in  $\sigma_{\text{tot}}(K^+p)$  with momentum. The new data for  $\pi^+p$  above 35 GeV/c are rather independent of momentum, showing a behaviour similar to that seen for  $\sigma_{\text{tot}}(\pi^+p)$  [1,2]. The data for pp are extremely flat, showing no momentum dependence above 35 GeV/c. It is possible that the  $\pi^+p$  and pp total cross sections have a minimum in the momentum region 50-100 GeV/c.

The same gross-features are seen in the data on deuterons and in the derived cross-sections on neutrons. It is notable that  $\sigma_{\text{tot}}(pn)$  is almost identical in magnitude with  $\sigma_{\text{tot}}(pp)$  in agreement with isospin independence [16]. For the pion-nucleon system this is not the case in the momentum range studied as is clearly shown by the comparison of  $\sigma_{\text{tot}}(\pi^+p)$  in fig. 2. For the  $K^+$ -nucleon system, the systematic errors are comparable with the difference between  $K^+n$  and  $K^+p$  cross-sections so no definite conclusion can be drawn.

Fig. 2 shows a comparison between the available data on total cross-sections for both particles and antiparticles on protons, plotted against the incident momentum. This figure suggests that the total cross-section for  $K^+p$  will approach the asymptotic value from below, unless the cross-section oscillates in value. The particle and antiparticle cross-sections are significantly different even at 60 GeV/c.

Fig. 3 shows the behaviour of the difference in total cross-sections for particle and antiparticle on protons ( $\Delta\sigma$ ) as a function of incident momentum  $p$ . In the region studied  $\Delta\sigma$  falls linearly on a log-log graph. This dependence may be described by:

$$\Delta\sigma = A p^{-n} \quad (4)$$

The straight lines in fig. 3 are least-square fits to the data and lead to the values of the coefficients  $A$  and  $n$  shown in table 3. This behaviour of the cross-section differences is consistent with the Pomeranchuk theorem [17], according to which  $\Delta\sigma \rightarrow 0$  as  $p \rightarrow \infty$ .

The fact that the  $K^+p$  total cross-section increases with momentum and thus the difference  $\Delta\sigma$  for  $K^+p$  decreases means the cross-section for regeneration of  $K^0$  must fall rather rapidly with momentum.

We gratefully acknowledge the cooperation of many IHEP people who ensured the successful operation of the accelerator and of the secondary beam channel and the support of Professors A. A. Logunov, R. M. Sulyaev and A. A. Naumov.

### References

- [1] J. V. Allaby, Yu. B. Bushnin, Yu. P. Gorin, S. P. Denisov, G. Giacomelli, A. N. Diddens, R. W. Dobinson, S. V. Donskov, A. Klovning, A. I. Petrukhin, Yu. D. Prokoshkin, C. A. Stahlbrandt, D. A. Stoyanova and R. S. Shuvalov, Preprint IHEP-69-87, Serpukhov (1969); Phys. Letters 30B (1969) 500; Yadern. Fiz. 12 (1970) 538.
- [2] S. P. Denisov, Yu. P. Dmitrevski, S. V. Donskov, Yu. P. Gorin, Au. M. Melnik, A. I. Petrukhin, Yu. D. Prokoshkin, V. S. Seleznev, R. S. Shuvalov, D. A. Stoyanova and L. M. Vasiljev, Preprint IHEP-71-48, Serpukhov (1971); Invited Report by Yu. D. Prokoshkin, 15th Intern. Conf. on High energy physics, Kiev (1970).
- [3] N. I. Golovnja, M. I. Grachev, K. I. Gubrienko, E. V. Eremenko, V. N. Zapolski, V. I. Kotov, Yu. D. Prokoshkin, V. S. Seleznev and Yu. S. Khodirev, Preprint IHEP, 71-46, Serpukhov (1971).
- [4] Yu. P. Gorin, S. P. Denisov, S. V. Donskov, V. I. Kotov, A. I. Petrukhin, Yu. D. Prokoshkin, V. S. Seleznev, D. A. Stoyanova, Yu. S. Khodirev and R. S. Shuvalov, Preprint IHEP 71-30, Serpukhov (1971).
- [5] S. P. Denisov, S. V. Donskov, Yu. P. Gorin, R. N. Krasnokutsky, A. I. Petrukhin, Yu. D. Prokoshkin, R. S. Shuvalov and D. A. Stoyanova, Preprint IHEP 70-48, Serpukhov (1970), Pribori i Tech. Exp. 2 (1971) 87; Nucl. Instr. Meth. 92 (1971) 77.
- [6] S. P. Denisov, S. V. Donskov, A. F. Dunaitsev, Yu. P. Gorin, A. I. Petrukhin, Yu. D. Prokoshkin, R. S. Shuvalov and D. A. Stoyanova, Preprint IHEP 69-63, Serpukhov (1969), Pribori i Tech. Exp. 3 (1970) 117, Nucl. Instr. Meth. 85 (1970) 101.
- [7] R. J. Tapper, Rutherford Laboratory Report NIRL/R/95 (1965).

- [8] V. D. Bartenev, G. G. Beznogikh, A. Buyak, K. I. Iovchev, L. F. Kirillova, P. K. Markov, B. A. Morozov, V. A. Nikitin, P. V. Nomokonov, U. K. Pilipenko, A. Sandach, M. G. Shafranov, V. A. Sviridov, Truong Bien, V. I. Zayachki, N. K. Zhidkov and L. S. Zolin, Invited Report by V. A. Nikitin, 15th Intern. Conf. on High energy physics, Kiev (1970).
- [9] G. Giacomelli, Progress in Nuclear Physics 12 (1970) 77.
- [10] K. G. Boreskov, A. M. Lapidus, S. T. Suchorukov and K. A. Ter-Martirosyan; Contributed paper to the 15th Intern. Conf. on High energy physics, Kiev (1970).
- [11] R. J. Glauber, Phys. Rev. 100 (1955) 242; V. Franco and R. J. Glauber, Phys. Rev. 142 (1966) 1195.
- [12] V. N. Gribov, JETP 56 (1969) 892; G. Alberi, L. Bertocchi and P. J. R. Soper, Phys. Letters 32B (1970) 367; V. V. Anisovitch, P. E. Volkovitsky and L. G. Dachno, Preprint IHEP, 71-9, Serpukhov (1971).
- [13] K. J. Foley, R. S. Jones, S. J. Lindenbaum, W. A. Love, S. Ozaki, E. D. Plainer, C. A. Quarles and E. H. Willen, Phys. Rev. Letters 19 (1967) 330; 19 (1967) 857.
- [14] W. Galbraight, E. W. Jenkins, J. F. Kycia, B. A. Leontic, R. H. Phillips, A. L. Read and R. Rubinstein, Phys. Rev. 138B (1965) 913.
- [15] Aachen-Berlin-CERN-London-Vienna and Bruxelles-CERN collaborations, J. V. Beupre et al. Preprint CERN 70-52 (1971).
- [16] L. B. Okun' and I. Ya. Pomeranchuk, Zh. Eksp. i Teor. Fiz. 30 (1956) 307; Soviet Phys. JETP 3 (1956) 307.
- [17] I. Ya. Pomeranchuk, Zh. Exp. i Teor. Fiz. 34 (1958) 725; Soviet Phys. JETP 7 (1958) 499.

\* \* \* \* \*